Pergamon

0094-5765(94)00262-2

Acta Astronautica Vol. 35, No. 2/3, pp. 167–174, 1995

0095-5765/95 $9.50 + 0.00

DYNAMICAL MODELLING AND CONTROL OF A SPACECRAFT-MOUNTED MANIPULATOR CAPTURING A SPINNING SATELLITE†

XAVIER CYRIL

CAE Electronics Ltd, P.O. Box 1800, St Laurent, Quebec, Canada H4L 4X4

and

GILBERT J. JAAR and ARUN K. MISRA

Department of Mechanical Engineering, McGill University, 817 Sherbrooke Street West, Montreal, Quebec, Canada H3A 2K6

Abstract—Issues associated with the modelling and control of a spacecraft-mounted manipulator capturing a spinning satellite are presented. The Lagrangian formulation is used to derive the dynamical equations of the system immediately following the capture. The formulation is carried out by writing Lagrange's equations for the individual bodies, and then assembling them to obtain the constrained dynamical equations of the system. The non-working constraint forces/torques are then eliminated by using the natural orthogonal complement which produces a set of independent dynamical equations. A control algorithm whose objective is to produce a set of feedback-linearized, homogeneous and uncoupled equations is designed and implemented. The initial conditions of the state variables needed to achieve smooth berthing of the satellite are computed, and the dynamics simulation of both the controlled and uncontrolled systems is carried out. The manipulator's structural flexibility is included in the dynamics simulation model.

1. INTRODUCTION

Future space missions will require the capture, retrieval and maintenance of satellites in orbit. This will be accomplished by means of robotic manipulators mounted on free-flying spacecraft which will be used to manipulate a satellite whose mass may be substantial compared to that of the spacecraft. The shuttle remote manipulator is a prime example of such a system. Docking berthing systems (DBS), which will be used in conjunction with the Space Shuttle, are being investigated [1], and involve simulations of the final approach, rendezvous and contact phases with the satellite to be captured.

A particular problem studied by several researchers is the dynamic coupling between the manipulator's links, the spacecraft and the payload. Due to this coupling, dynamic forces and torques will be exerted on both the spacecraft and the payload, which will cause them to rotate and translate relative to their respective orbital frames. These movements, which could be large depending on the relative masses of the system's components, are undesirable since they may involve a large end-effector motion and an attitude drift of the spacecraft. The manipulator's workspace will be reduced as well [2].

Another research concern is the structural flexibility of the manipulator links, which becomes significant when manipulating large payloads, and/or operating at high speeds. The effect of structural flexibility on the behaviour of the entire system has been extensively studied. It was found that such vibrations are so substantial that they might tumble the spacecraft on which the manipulator is mounted [3]. The effect of both joint and link flexibility on the dynamic stability of the system has also been investigated, and found to be quite significant. They are the sources of trajectory tracking errors and undesirable oscillations of the end effector [4]. Flexibility in both the platform and the payload has been considered as well [5].

Control of space manipulators poses a challenge to the control system designer. This is due to the highly non-linear equations of motion and the strong coupling between its generalized co-ordinates. In [6] the authors propose the use of reaction wheels and/or jet thrusters to control the spacecraft attitude and position by cancelling the force and torque disturbances caused by the manipulator and the manipulated payload. Another scheme [7] proposes an active attitude control system (ACS) that maintains the spacecraft's attitude relative to its orbital frame, which is achieved by applying appropriate corrective torques. The spacecraft's center of mass, however, is still free to translate in response to the force disturbances of the manipulator and its payload. In [8] the authors

†Paper IAF-92-29 presented at the *43rd Astronautical Congress*, Washington, D.C., U.S.A., 28 August–5 September 1992.

propose a feedback linearization control for the accurate positioning of the end-effector. Very few researchers have investigated the effect of capturing a satellite. In [9] the problem is formulated, however, the post-capture dynamics was not simulated.

The purpose of this paper is to study the effect of capturing a spinning satellite in orbit with a given spin rate, on the dynamics of the manipulator and the spacecraft. The spin rate will govern the behaviour of the system just after the capture. First, the dynamics simulation of the uncontrolled system is carried out. In light of the simulation results, a control scheme is designed and implemented in order to control both the attitude of the spacecraft and the payload, in addition to the position and rates of the manipulator joints. A non-linearity compensation and decoupling proportional-derivative (PD) control torque is used. Throughout the analysis the position of the spacecraft's centre of mass is assumed to be maintained in the initial circular orbit.

2. FORMULATION OF THE PROBLEM

In this section the dynamical equations of the system are derived using the Lagrangian formulation. Contrary to the usual practice in Lagrangian dynamics, where the equations for the system as a whole are derived, the Lagrange equations are derived here for each body and then asembled to obtain the equations of motion for the system. This method, however, introduces the non-working constraint forces/torques which will be eliminated by using the *natural orthogonal complement* [10].

The system under investigation is illustrated in Fig. 1. It is composed of a main body (hereafter referred to as spacecraft) that serves as a platform on which a two-link robotic manipulator is mounted, and a payload. It is important to note that although the manipulator shown consists of two links the formulation developed is applicable to multi-link manipulator.

If we represent the system under investigation as an N-body system then the vector containing its independent generalized co-ordinates (ψ) can be defined as:

$$\psi = [\psi_1^T, \psi_2^T, \ldots, \psi_N^T]^T \tag{1}$$

where ψ_1 represents the spacecraft's attitude degrees of freedom, namely, pitch, roll and yaw. It can be written as:

$$\psi_1 = [\alpha, \beta, \gamma]^T \tag{2}$$

where $\alpha = \theta_1$ and $\beta = \gamma = 0$ for the planar case.

For the remaining $N-1$ bodies, the generalized co-ordinates depend on whether the body is rigid or flexible

$$\text{flexible} \quad \psi_1 = [\theta_i, \mathbf{b}_i]^T \tag{3}$$

$$\text{rigid} \quad \psi_i = [\theta_i] \tag{4}$$

where

$$\mathbf{b}_i = [b_{i1}, b_{i2}, \ldots, b_{im}] \tag{5}$$

contains the m generalized co-ordinates associated with bending in link i, and θ_i is the angle of rotation of joint i. The angle between X_i and X_{i-1} is the sum of θ_i and the tip rotation of link $(i-1)$.

The system shown in Fig. 1 consists of four-bodies. The orbital and system frames are located at the

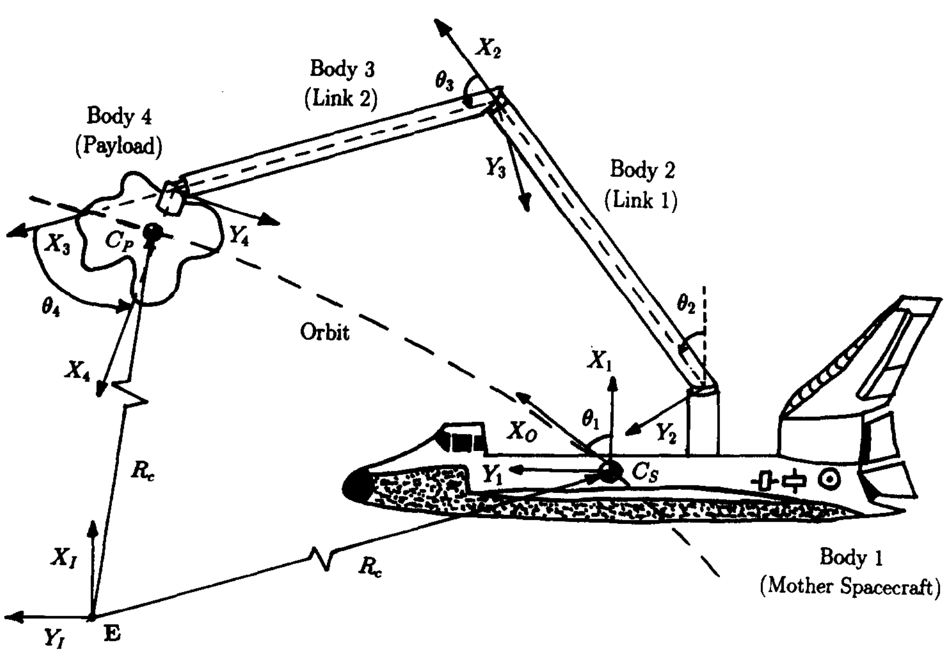

Fig. 1. System description and the reference frames.

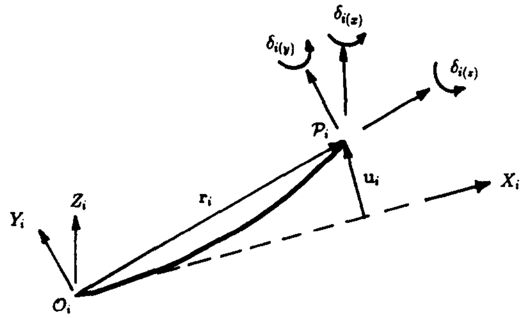

Fig. 2. Flexible link.

spacecraft's centre of mass C_S. At a given instant, the orientation of the body fixed frame (X_1, Y_1, Z_1) relative to the orbital frame (X_0, Y_0, Z_0) defines the spacecraft's attitude, represented by the pitch, roll and yaw angles. The angular velocity of the orbital frame with respect to the inertial frame (X_I, Y_I, Z_I) located at the Earth's centre, is denoted by Ω.

Let $\mathbf{r}_i$ be the position vector of any point P on the *flexible* body with respect to (X_i, Y_i, Z_i). A set of unit vectors $\mathbf{x}_i, \mathbf{y}_i, \mathbf{z}_i$ are chosen to be parallel to (X_i, Y_i, Z_i), respectively and x_i, y_i, z_i are the co-ordinates of a point in the frame. Vector $\mathbf{r}_i$ could be written as

$$\mathbf{r}_i = x_i\mathbf{x}_i + \mathbf{u}_i(x_i, t) \tag{6}$$

where $\mathbf{u}_i$ is the displacement vector due to the bending of body i. The flexible links are modelled as Euler–Bernoulli beams. The stiffening effect due to the axial shortening is ignored since the links will be moved at low speeds. The deformations of the flexible link are described by appropriate modal shape functions and time-dependent generalized co-ordinates. The displacement vector $\mathbf{u}_i$ can be written in the compact form:

$$\mathbf{u}_i(x_i, t) = \mathbf{B}_i(x_i)\mathbf{b}_i(t) \tag{7}$$

where $\mathbf{B}_i$ is the matrix of shape functions associated with bending of link i.

The rotation of the tip of link i with respect to (X_i, Y_i, Z_i) due to the flexibility is denoted by $\boldsymbol{\delta}_i$ (Fig. 2). The position of the origin of (X_i, Y_i, Z_i) with respect to that of (X_0, Y_0, Z_0) is given by:

$$\mathbf{p}_i = \mathbf{p}_{i-1}(l_{i-1}) + \mathbf{r}_i(l_{i-1}) \tag{8}$$

The angular velocity of (X_i, Y_i, Z_i) with respect to (X_0, Y_0, Z_0) can be shown to be:

$$\omega_i = \omega_{i-1} + \dot{\boldsymbol{\delta}}_{i-1} + \dot{\boldsymbol{\theta}}_i\mathbf{z}_i \tag{9}$$

The kinetic energy of body i, denoted as T_i can be written in the form:

$$T_i = T_i(\mathbf{q}_i, \mathbf{v}_i) = \tfrac{1}{2}\mathbf{v}_i^{\mathrm{T}}\mathbf{M}_i(\mathbf{q}_i, t)\mathbf{v}_i \tag{10}$$

where $\mathbf{M}_i$ is the *extended* inertia matrix of the dynamical system. Here extended refers to quantities which comprise both rotational and translational variables or parameters of the body.

The *extended* position vector, $\mathbf{q}_i$, is defined as:

$$\text{flexible} \quad \mathbf{q}_i = [\mathbf{p}_i^{\mathrm{T}}, \hat{\mathbf{q}}_i^{\mathrm{T}}, \mathbf{b}_i^{\mathrm{T}}]^{\mathrm{T}} \tag{11}$$

$$\text{rigid} \quad \mathbf{q}_i = [\mathbf{p}_i^{\mathrm{T}}, \hat{\mathbf{q}}_i^{\mathrm{T}}]^{\mathrm{T}} \tag{12}$$

where $\hat{\mathbf{q}}_i$ is the quaternion representing the orientation of body i-fixed frame.

The *extended* velocity vector, $\mathbf{v}_i$ is defined as:

$$\text{flexible} \quad \mathbf{v}_i = [\dot{\mathbf{p}}_i^{\mathrm{T}}, \omega_i^{\mathrm{T}}, \dot{\mathbf{b}}_i^{\mathrm{T}}]^{\mathrm{T}} \tag{13}$$

$$\text{rigid} \quad \mathbf{v}_i = [\dot{\mathbf{p}}_i^{\mathrm{T}}, \omega_i^{\mathrm{T}}]^{\mathrm{T}} \tag{14}$$

The potential energy of body i, denoted by U_i, is a function of the extended position vector $\mathbf{q}_i$ alone. It consists of two parts; one due to the gravity gradient and the other due to the elastic strain energy stored in the flexible body. The effect of the former is much smaller than the latter and is neglected here. Hence the potential enrgy of a rigid body is equal to zero.

The dynamical equations of motion of body i can be derived using the Lagrangian formulation, which is given by the following expression:

$$\frac{\mathrm{d}}{\mathrm{d}t}\left(\frac{\partial T_i}{\partial \dot{\mathbf{q}}_i}\right) - \frac{\partial T_i}{\partial \mathbf{q}_i} = \boldsymbol{\chi}_i - \frac{\partial U_i}{\partial \mathbf{q}_i} \tag{15}$$

where $\boldsymbol{\chi}_i$ contains the dissipative, external, and constraint forces/torques on body i.

Upon assembling the equations of motion for each body, the system's constrained equations of motion can be written in the form:

$$\mathbf{M}\dot{\mathbf{v}} = \boldsymbol{\phi}^{\mathrm{E}} + \boldsymbol{\phi}^{\mathrm{S}} + \boldsymbol{\phi}^{\mathrm{C}} \tag{16}$$

where

$$\mathbf{M} = \mathrm{diag}(\mathbf{M}_1, \mathbf{M}_2, \ldots, \mathbf{M}_N) \tag{17}$$

is the generalized extended inertia matrix and $\mathbf{v}$, $\boldsymbol{\phi}^{\mathrm{E}}$, $\boldsymbol{\phi}^{\mathrm{S}}$ and $\boldsymbol{\phi}^{\mathrm{C}}$, represent the generalized extended velocity vector, and the generalized external, system and contraint forces of the system, respectively.

The natural orthogonal complement, $\mathbf{N}$, is defined as the matrix which transforms the independent generalized velocities to extended velocities and is obtained from

$$\mathbf{v} = \mathbf{N}(\dot{\boldsymbol{\psi}} + \dot{\boldsymbol{\psi}}_0) \tag{18}$$

where $\dot{\boldsymbol{\psi}}$ is the generalized velocity of the system and $\dot{\boldsymbol{\psi}}_0$ is the vector containing the orbital rate Ω of the system. It is proven [10] that upon the premultiplication of eqn (16) by $\mathbf{N}^{\mathrm{T}}$ the constraint force vector $\boldsymbol{\phi}^{\mathrm{C}}$ could be eliminated. Furthermore, an expression for $\dot{\mathbf{v}}$ is obtained as follows

$$\dot{\mathbf{v}} = \mathbf{N}\ddot{\boldsymbol{\psi}} + \dot{\mathbf{N}}(\dot{\boldsymbol{\psi}} + \dot{\boldsymbol{\psi}}_0) \tag{19}$$

where

$$\dot{\boldsymbol{\psi}}_0 = [\Omega, 0, \ldots, 0] \tag{20}$$

Upon pre-multiplication of eqn (16) by $\mathbf{N}^T$ and the substitution of eqn (19), the independent dynamical equation of motion of the system becomes:

$$\tilde{\mathbf{M}}\ddot{\boldsymbol{\psi}} = \mathbf{c}(\boldsymbol{\psi}, \dot{\boldsymbol{\psi}}, \dot{\boldsymbol{\psi}}_0) + \mathbf{f} \tag{21}$$

where

$$\tilde{\mathbf{M}} = \mathbf{N}^T\mathbf{M}\mathbf{N}$$

$$\mathbf{c} = \mathbf{N}^T[\boldsymbol{\psi}^S - \mathbf{M}\dot{\mathbf{N}}(\dot{\boldsymbol{\psi}} + \dot{\boldsymbol{\psi}}_0)]$$

$$\mathbf{f} = \mathbf{N}^T\boldsymbol{\psi}^E$$

In the above equation, $\tilde{\mathbf{M}}$ is the generalized mass matrix of the system, which is symmetric and positive definite. Vector $\mathbf{f}$ represents the genealized external forces, and the vector $\mathbf{c}$ contains the Coriolis, damping and centrifugal terms.

It is more convenient for simulation and control to partition eqn (21) into rotational and elastic co-ordinates dependent matrices and vectors as follows

$$\begin{bmatrix} \tilde{\mathbf{M}}_{\theta\theta} & \tilde{\mathbf{M}}_{\theta b} \\ \mathbf{M}_{b\theta} & \mathbf{M}_{bb} \end{bmatrix} \begin{bmatrix} \ddot{\boldsymbol{\theta}} \\ \ddot{\mathbf{b}} \end{bmatrix} = \begin{bmatrix} \mathbf{c}_\theta \\ \mathbf{c}_b \end{bmatrix} + \begin{bmatrix} \boldsymbol{\tau} \\ 0 \end{bmatrix} \tag{22}$$

where the subscripts θ and b represent matrices and vectors related to the rotational and bending degrees of freedom, respectively. The upper part of the external generalized forces vector is equal to τ which corresponds to the nominal joint torques. The lower part, however, is noted to be equal to zero, which implies that actuators are only present at the joints and separate generalized forces cannot be applied to control the flexible modes.

3. CONTROL DESIGN AND IMPLEMENTATION

The objective of the control system is to maintain stability following the capture of a spinning satellite. The captured satellite is considered as deterministic disturbance, i.e. the inertia and dynamic properties are assumed to be known.

The control method used in this paper is the computed torque method in which the equations of motion are linearized via feedback. Therefore, this control method is sometimes referred to as feedback linearization control. The required torques could be calculated based on the sensor measurements. The control scheme will be first implemented by assuming that the manipulator is rigid. Next, the effect of flexibility will be evaluated and incorporated in the control design.

For rigid link manipulators, the joint angles and their rates are measured by colocated sensors at the joints. By setting all the flexibility related matrices in (22) to zero, the equation of motion for the rigid system can be written as

$$\tilde{\mathbf{M}}_{\theta\theta}\ddot{\boldsymbol{\theta}} = \mathbf{c}_\theta + \boldsymbol{\tau} \tag{23}$$

The joint actuator torques required to suppress the disturbance need to be calculated. A simple feedback linearization control law is designed, and can be written in the form

$$\boldsymbol{\tau} = -\tilde{\mathbf{M}}_{\theta\theta}[\mathbf{D}_1\dot{\boldsymbol{\theta}} + \mathbf{D}_2(\boldsymbol{\theta} - \boldsymbol{\theta}_d)] - \mathbf{c}_\theta \tag{24}$$

where

$$\mathbf{D}_1 = \mathrm{diag}(2\zeta_1\omega_1, 2\zeta_2\omega_2, \ldots, 2\zeta_N\omega_N)$$

and

$$\mathbf{D}_2 = \mathrm{diag}(\omega_1^2, \omega_2^2, \ldots, \omega_N^2)$$

are diagonal matrices containing the control gains, and $\boldsymbol{\theta}_d$ contains the desired final values of the joint angles and their rates. It must be noted that vector $\mathbf{c}_\theta$ in eqn (24) represents the non-linear compensation term.

By substituting eqn (24) into eqn (23), a set of linearized, uncoupled and homogeneous equations of motion are obtained and could be written as

$$\ddot{\boldsymbol{\theta}} + \mathbf{D}_1\dot{\boldsymbol{\theta}} + \mathbf{D}_2(\boldsymbol{\theta} - \boldsymbol{\theta}_d) = 0 \tag{25}$$

For flexible-link manipulators, however, the control is not as straightforward because it involves the elastic degrees of freedom. Also, measurement of the angle between two links at a joint represents the sum of the angle between the two co-ordinate frames and the slopes of the elastic deformations $\boldsymbol{\delta}$ (Fig. 2) at the joints.

There can be three approaches for the flexible system control:

(1) Elastic effects are ignored, i.e. the equation of motion is assumed to be as in (23). The torque computed by this model would give good results only if the elastic effects are negligible, otherwise it may result in gross inaccuracies in the positioning of the end-effector.
(2) The elastic effects are included in the mathematical model, and their amplitudes could be determined from the sensor readings by means of an estimator. This model treats the elastic deformations as known disturbances, but does not explicitly control them.
(3) Active control of both the rotational and bending co-ordinates, which is achieved by applying both torques and generalized forces. Such control is possible only if actuators capable of applying transverse forces to the links are present. Additionally, measurements of the elastic generalized co-ordinates and their rates must be available.

The approach presented in item (3) above is still in the experimental stages and has not been used in an actual situation. Therefore, the only feasible model is the one presented in item (2). The bending co-ordinates could be solved for in terms of the rotational co-ordinates and equation (22) could be re-arranged as:

$$\widehat{\mathbf{M}}\ddot{\boldsymbol{\theta}} = \hat{\boldsymbol{c}} + \boldsymbol{\tau} \tag{26}$$

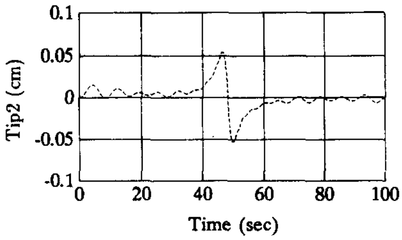

Fig. 3. Tip_2 deflection (——, rigid; . . . , flexible).

where

$$\widehat{\mathbf{M}} = \tilde{\mathbf{M}}_{\theta\theta} - \tilde{\mathbf{M}}_{\theta b}\tilde{\mathbf{M}}_{bb}^{-1}\mathbf{M}_{b\theta}$$

$$\hat{\mathbf{c}} = \mathbf{c}_\theta - \tilde{\mathbf{M}}_{\theta b}\tilde{\mathbf{M}}_{bb}^{-1}\mathbf{c}_b$$

The **PD** control torque that produces an equation of controlled motion similar to (25) is

$$\boldsymbol{\tau} = -\widehat{\mathbf{M}}[\mathbf{D}_1\dot{\boldsymbol{\theta}} + \mathbf{D}_2(\boldsymbol{\theta} - \boldsymbol{\theta}_d)] - \hat{\mathbf{c}} \tag{27}$$

The control torque vector in eqn (27) is of the same order as the rigid-body degrees of freedom, consequently a similar control strategy could be used for the flexible and rigid systems.

Another simplified control scheme whose objective is to control the attitude of the space craft only is also investigated. It is noted that $\tilde{\mathbf{M}}_{1j} = 0$ for $j \neq 1$. Thus, the individual equation of motion of the spacecraft can be written in the form

$$I_1\ddot{\theta}_1 = \tau_1 + F_1(\psi, \dot{\psi}, \dot{\psi}_0) \tag{28}$$

where I_1 represents the moment of inertia of the spacecraft about its centre of mass and F_1 contains the non-linear terms.

Due to the absence of inertia coupling in eqn (28), a simple **PD** control torque could be applied to achieve attitude control of the spacecraft. The feedback-linearization control torque can be expressed as

$$\tau_1 = -I_1(2\zeta_1\omega_1\dot{\theta}_1 + \omega_1^2\theta_1) - F_1 \tag{29}$$

where ζ_1 and ω_1 are appropriate control gains. By substituting eqn (29) into eqn (28) the equation of motion of the spacecraft can be written as

$$\ddot{\theta} + 2\varsigma_1\omega_1\dot{\theta}_1 + \omega_1^2\theta_1 = 0 \tag{30}$$

4. SIMULATION RESULTS AND DISCUSSION

A two-link spacecraft-mounted flexible manipulator (Fig. 1) is used in the simulation. The spacecraft to payload mass ratio is 10 and the payload has an initial spin rate of $\frac{1}{2}$ rpm. The manipulator parameters are identical to those of the shuttle remote manipulator [10]. The flexibility of each link is modelled by one mode only.

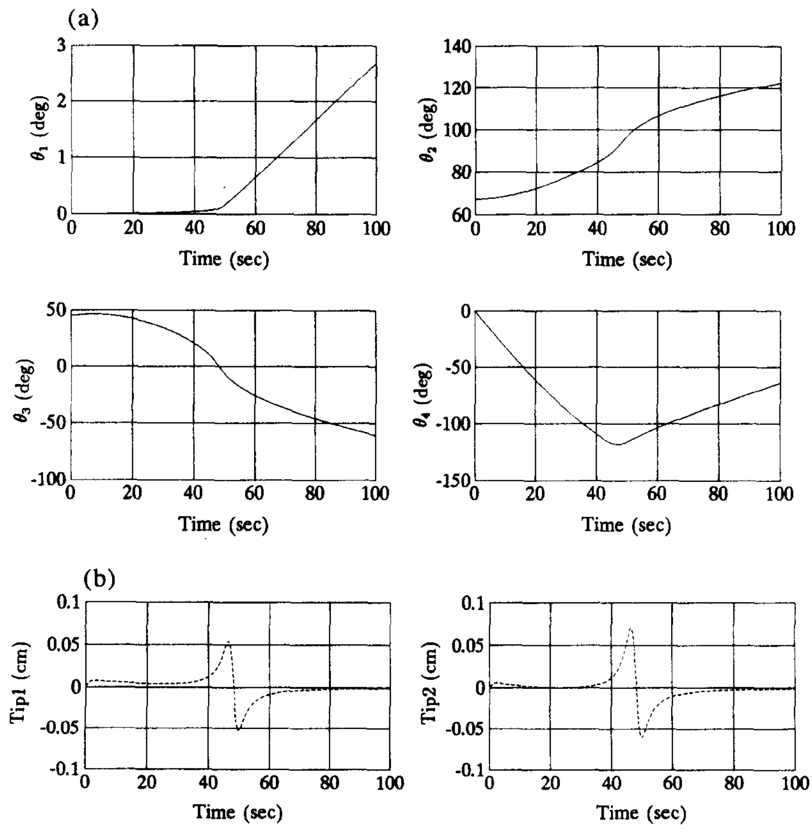

Fig. 4. (a) Joint angles of the uncontrolled system. (b) Tip deflections of the uncontrolled system (——, rigid; . . . , flexible).

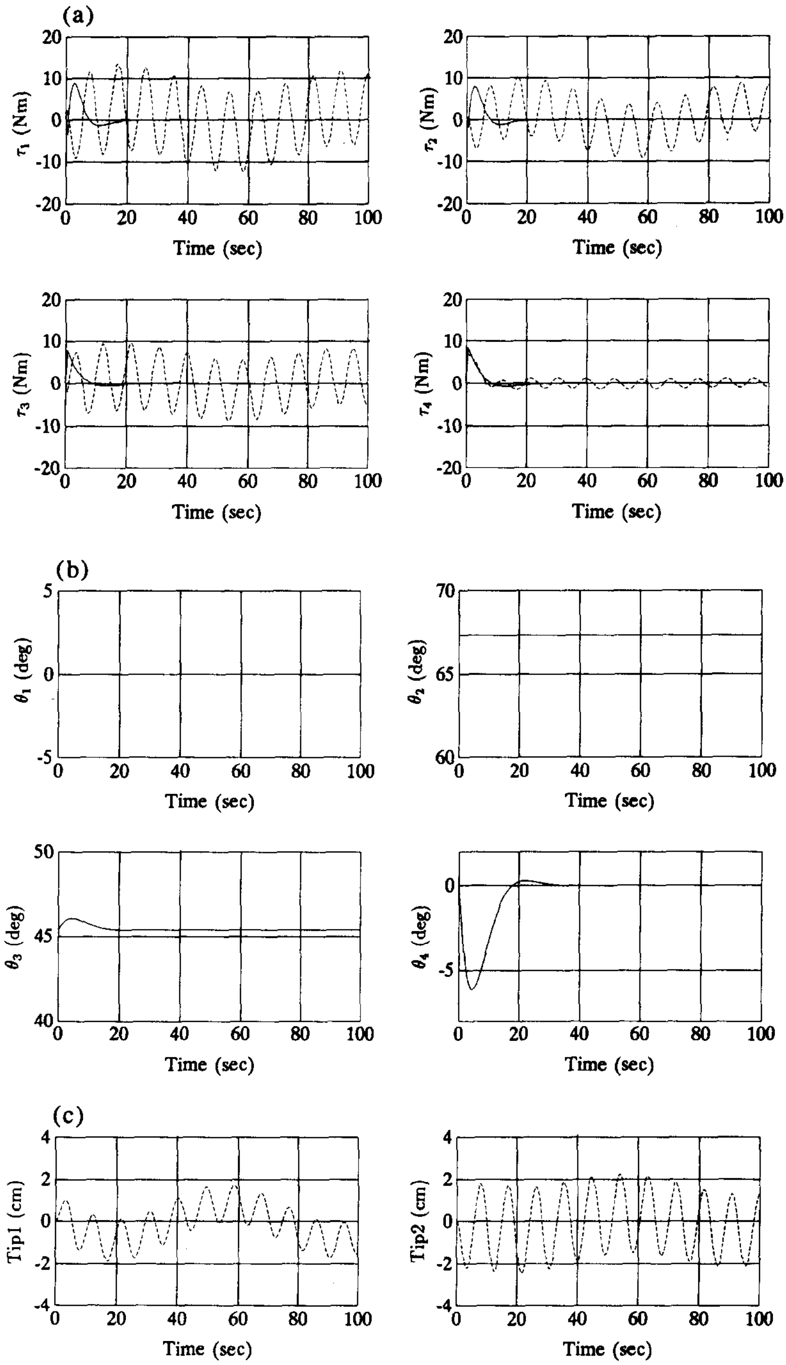

Fig. 5. (a) Joint torques of the controlled system. (b) Joint angles of the controlled system. (c) Tip deflections of the controlled system (——, rigid; . . . , flexible).

The initial values of the state variables are calculated by solving the inverse kinematics problem. The objective is to achieve smooth berthing of the payload as it is captured by the end-effector of the robotic manipulator.

First, a dynamical simulation of the uncontrolled system after capture is carried out. The tip deflection of the second link (Fig. 3) shows a steady oscillatory behaviour. This is because the flexible response does not account for energy dissipation due to the links' deformations. Hence, structural damping is incorporated in the flexible link model. The simulation of the uncontrolled system is then repeated and the results are shown in Figs 4(a) and (b). It is found that, without control, the spacecraft's pitch angle drifts by almost 3° in 100 s. Furthermore, the end-effector reaches a maximum rotation of 120 deg in 45 seconds which will probably cause breakage. The tip deflection of the flexible links (Fig. 4b) are quite reasonable and the oscillations damp out fairly quickly due to the incorporation of structural damping in the model.

Next, a simulation is carried out using the feedback linearization control torque whose purpose is to control the rotational degrees of freedom only. The torques calculated are shown in Fig. 5(a) where eqn (24) is used for the rigid system, and eqn (27) is used for the flexible system. The response of the dynamical system to the applied corrective torques [Fig. 5(b) and (c)] is very good and the desired final values of the rotational co-ordinates are attained. The spacecraft pitch is maintained at zero throughout the similation period, while the end-effector rotates only 7° before the rotation is reduced to zero. The link joint angles reach steady state fairly quickly, and the final configuration of the system is identical to the initial one; this is due to the position tracking in the control law. It is noted that the application of joint torques excites the elastic modes of the links, which is evident in the oscillatory behaviour of the tip deflection of the links [Fig. 5(c)]. It is found that the inclusion of structural damping in the model has some effect on damping out the tip oscillations, however, a more effective control could only be achieved by the application of transverse control forces along the links by means of distributed actuators. The oscillatory nature of the control torques is expected because they are designed to compensate for the non-linear terms, which, after the rotational co-ordinates are controlled, are a function of the flexible co-ordinates only. Such oscillations would only damp out if the flexible co-ordinates are explicitly controlled.

Finally, a simulation whose objective is to only control the attitude of the spacecraft is carried out by implementing the control torque calculated using eqn (29). The results of the simulation are shown in Fig. 6. It is found that the response of the spacecraft agrees with the theoretical expectations due to the absence of inertia coupling in its equation of motion (25). The response of both the flexible and rigid systems to the control torque is quite close, and the spacecraft pitch drifts by only 0.07° before it settles down with a very small steady state error. Due to the small magnitude and the short duration of the control torque, its effect on the joint angles and the link deflections (not shown in the plots) is negligible.

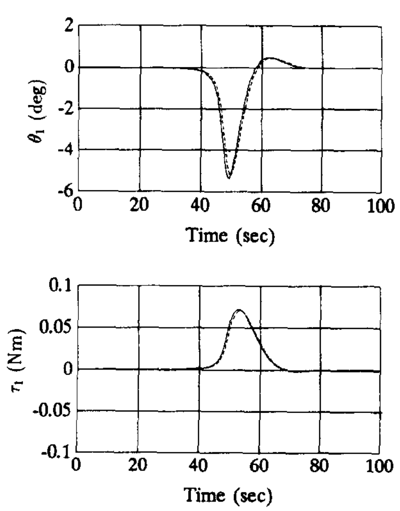

Fig. 6. Attitude control (——, rigid; . . . , flexible).

5. CONCLUSIONS

Based on the analysis, the following concluding remarks can be made:

(1) The effect of capturing a spinning satellite on the manipulator's dynamics response could be substantial depending on the mass and initial spin rate of the captured satellite.
(2) The effect of link flexibility further complicates the dynamical analysis of the system and could be large depending on the magnitude of the disturbance.
(3) A control law has to be designed and implemented in order to suppress the disturbance caused by the spinning satellite.
(4) The inclusion of structural damping in the dynamical model provides a more realistic response. Friction in the joints could be modelled as well in order to improve the transient response of the system and achieve steady state faster.
(5) The resonse of both the rigid and flexible dynamical system to the **PD** feedback-linearization control is satisfactory. However, the elastic co-ordinates, which are not explicitly controlled, are excited by those same torques.

Acknowledgements—The authors wish to express their gratitude to the Institute of Robotic and Intelligent Systems (IRIS) and the Natural Sciences and Engineering Research Council of Canada (NSERC) for providing the funding for this research.

REFERENCES

1. A. Tobias, F. Venditti and N. Cable, Docking berthing systems: functions and simulation. *Proceedings 2nd European In-Orbit Operations Technology Symposium*, Toulouse, France, 12–14 September, pp. 259–270 (1989).
2. Z. Vafa and S. Dubowski, On the dynamics of manipulators in space using the virtual manipulator approach. *Proceedings 1987 IEEE Conference on Robotics and Automation*, Rayleigh, NC, 30 March–3 April, pp. 579–585 (1987).
3. R. W. Longman, Attitude tumbling due to the flexibility in satellite-mounted robots. *J. Astronaut. Sci.* **38**, 487–509 (1990).
4. G. Yang and M. Donath, Dynamic model of a one-link robot manipulator with both structural and joint flexi-

bility. *IEEE International Conference on Robotics and Automation*, Philadelphia, PA, pp. 476–481 (1988).
5. J. K. Chan and V. J. Modi, A closed-form dynamical analysis of an orbiting flexible manipulator. *Acta Astronautica* **25**, 67–75 (1991).
6. M. Torres and S. Dubowsky, Path planning for space manipulators to minimize spacecraft attitude disturbance. *Proceedings 1991 IEEE International Conference on Robotics and Automation*, Sacramento, CA, Vol. 3, pp. 2522–2528, April (1991).
7. R. Longman, R. Lindberg and M. Zedd, Satellite-mounted robot manipulators—new kinematics and reaction moment compensation. *Int. J. Robot. Res.* **6**, 87–103 (1987).
8. H. Baruh and S. S. K. Tadikunda, Issues in the dynamics and control of flexible robot manipulators. *AIAA Symposium on Dynamics and Control of Large Structures*, 29 June–1 July, pp. 659–671 (1987).
9. K. Yoshida, R. Kurazume, N. Sashida and Y. Umetani, Modelling of collision dynamics for space free-floating links with extended generalized inertia tensor. *Proceedings IEEE International Conference on Robotics and Automation*, Nice, France, May (1992).
10. X. Cyril, J. Angeles and A. Misra, Dynamics of flexible multibody mechanical systems. *Trans. CSME* **15**, 235–256 (1991).